A New IIR Nyquist Filter with Zero Intersymbol Interference and Its Frequency Response Approximation

KENJI NAKAYAMA, MEMBER, IEEE, AND TOSHIHIKO MIZUKAMI

Abstract —A new infinite impulse response (IIR) Nyquist filter with zero intersymbol interference is proposed. The necessary and sufficient conditions for the transfer function are obtained. The proposed IIR Nyquist filter requires only frequency-domain optimization. Multistep optimization, using the iterative Chebyshev approximation, is proposed. This method is able to design a new kind of IIR Nyquist filter with the minimum order. Numerical examples for 30- and 15-percent rolloff rates are illustrated. From these examples, it is confirmed that the IIR approach can reduce the filter order and hardware size, compared with the conventional finite impulse response (FIR) Nyquist filters. Its efficiency becomes marked for high Q Nyquist filters.

Manuscript received November 12, 1980; revised June 1, 1981.
The authors are with the Transmission Division, Nippon Electric Company, Ltd., Kawasaki-City, 211 Japan.

I. Introduction

NYQUIST filters by which data spectrum is band limited and intersymbol interference becomes minimum, play a very important role in data transmission. Several kinds of design approachs for Nyquist filters have been proposed. In continuous time systems, Spaulding's method [1] using Temes–Gyi's transfer function [2] able to accomplish Chebyshev attenuation characteristics for the given poles, and the improved Spaulding's method proposed by Yoshida and Ishizaki [3], by which an effective stopband attenuation can be obtained, are very useful.

Recently, an advanced digital device technology has

0098-4094/82/0001-0023$00.75 ©1982 IEEE

promoted transmission system digitalization. Digital Nyquist filters become very important for such digital modem systems. There are two kinds of structures for digital filters, finite impulse response (FIR) filters and infinite impulse response (IIR) filters. IIR Nyquist filter designs can be obtained basically from that for continuous time filters through the Z-transformation [4]. Conventional IIR Nyquist filter design requires both time- and frequency-response optimization. Due to many all-pass sections used for time-response optimization, a filter order becomes high. Since sensitivity for an impulse response at the Nyquist rate is very high, large coefficient wordlengths are necessary. On the other hand, filter coefficient for FIR filters corresponds to an impulse response directly. Therefore, an exact zero crossing impulse response can be obtained, and intersymbol interference becomes exactly zero [5]–[7]. Coefficient roundoff is insensitive for a time response at the Nyquist rate and is not so sensitive for a frequency response. Therefore, coefficient wordlengths can be reduced. FIR filters, however, require high filter order for a high Q frequency response. Hence they are not so attractive for small rolloff rate Nyquist filters.

In this paper, a new IIR Nyquist filter design method is proposed, which has an exact zero crossing impulse response. Zero intersymbol interference and insensitive coefficient roundoff can be realized as well as FIR filters. Moreover, a filter order can be reduced sufficiently for small rolloff rate IIR Nyquist filters, compared with FIR Nyquist filters.

Section II provides necessary and sufficient conditions for an IIR transfer function with zero intersymbol interference. A design approach based on the above transfer function is discussed in Section III. Numerical examples for 30- and 15-percent rolloff rates are illustrated in Section IV. Section IV also discusses a comparison between FIR and the proposed IIR Nyquist filters with regard to computational complexity and quantization error.

II. IIR Transfer Function with Zero Intersymbol Interference

A. Necessary and Sufficient Conditions

Fig. 1 shows a block diagram and filter responses for Nyquist filters. $X(z^M)$ is the transform of data signal whose speed is the Nyquist rate f_N. The sampling rate for $H(z)$ and $Y(z)$ is f_s which is M times as high as f_N

$$f_s = Mf_N, \qquad M\text{: integer} \tag{1}$$

z is

$$z = e^{j\omega/f_s}. \tag{2}$$

Fig. 1(b) shows a frequency response, where

$$\Omega_p = \pi\frac{f_N}{f_s}(1-\rho) \tag{3a}$$

$$\Omega_c = \pi\frac{f_N}{f_s}(1+\rho) \tag{3b}$$

$$T = 1/f_s \tag{4}$$

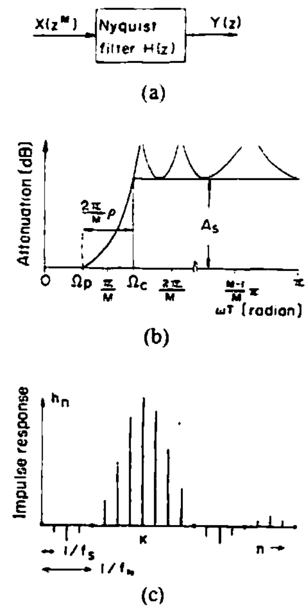

Fig. 1. Concept for Nyquist filters. (a) Block diagram. (b) Frequency response. (c) Impulse response.

ρ indicates the rolloff rate. Necessary and sufficient conditions by which an impulse response exactly zero crosses at the Nyquist rate except for one point, are given as a theorem in the following. The proof is given in Appendix.

Theorem

Necessary and sufficient conditions by which the impulse response h_n for $H(z)$ given by (5a) satisfies (5b) and (5c) are given by either (6)–(8) or (9)–(11).[1]

$$H(z) = \frac{\sum_{i=0}^{N_n} a_i z^{-i}}{\sum_{i=0}^{N_d} b_i z^{-i}}, \qquad b_0 = 1 \tag{5a}$$

$$h_n = 0, ((n-K))_M{}^2 = 0, \text{ and } n \neq K \tag{5b}$$

$$h_K \neq 0, \qquad K\text{: positive integer.} \tag{5c}$$

(A)

$$((N_d))_M = 0 \tag{6}$$

$$b_i = 0, \qquad ((i))_M \neq 0 \tag{7}$$

$$a_{K+kM} = a_K \cdot b_k, \qquad k\text{: integer} \tag{8a}$$

$$a_K \neq 0. \tag{8b}$$

(B)

$$((N_d))_M = M-1 \text{ and } b_1 \neq 0 \tag{9}$$

$$b_i = b_{M[\frac{i}{M}]} \cdot b_1^{((i))_M}{}^3 \tag{10}$$

$$a_{K+kM} - a_{K+kM-1} \cdot b_1 = \left(b_{kM} - b_{(k-1)M} \cdot b_1^M\right) \cdot (a_K - a_{K-1} \cdot b_1), \qquad k\text{: integer} \tag{11a}$$

[1]The former and latter conditions are called as Types A and B, respectively, in the following discussion.

[2]$((\cdot))_M$ is modular operation with mod M.

[3]$[R]$ denotes the maximum integer not exceeding R where R is assumed to be a real value.

$$a_K - a_{K-1} \cdot b_1 \neq 0. \qquad (11b)$$

The conditions $h_i = 0$ for $i<0$, $a_i = 0$ for $i<0$ and $N_n < i$, and $b_i = 0$ for $i<0$ and $N_d < i$ are tacitly held in this paper.

B. Constraints on Zero-Pole Locations

The necessary and sufficient conditions for a_i and b_i cause some constraints on zero-pole locations.

Type A

The denominator is a polynomial of z^{-M}. Therefore, poles become Mth order and are periodically located with period $2\pi/M$. All numerator coefficients cannot be determined independently. $a_{K+kM}(k\neq 0)$ takes a value which is zero or depends on the denominator coefficients. The number of dependent numerator coefficients is $[K/M] + [(N_n - K)/M]$. It means that the same number of zeros are automatically determined after the rest of the zeros and the denominator are given. Generally speaking, it is difficult to control the dependent zero locations using the independent parameters.

Type B

The denominator can be factorized into the two polynomials $Q_1(z)$ and $Q_2(z^M)$ as mentioned in Appendix. $Q_2(z^M)$ is a polynomial of z^{-M}, and has the same kind of pole as in Type A. $Q_1(z)$ is a polynomial factor of $1 - b_1^M z^{-M}$, and its pole is expressed by

$$z_i = b_1 e^{j\frac{2\pi i}{M}}, \qquad i = 1,2,\cdots,M-1. \qquad (12)$$

In the numerator polynomial, independent and dependent zeros exist as well as in Type A.

These constraints on the zero-pole locations have to be taken into account in filter design procedures. The poles given by $Q_1(z)$ in Type B, are located at stopband, and do not contribute passband shaping. Consequently, Type B is not suited to frequency-response optimization compared with Type A.

C. Optimum Configuration for Nyquist Filters

As previously mentioned, the input and output signal rates for a Nyquist filter are f_N and $f_s(=Mf_N)$, respectively. It is considered as a signal rate transformation. Computational complexity for such a filter can be reduced by constructing a filter in a parallel form using low rate subfilters. Configurations for Types A and B are described in the following.

Type A

From the conditions given by the Theorem, the transfer function can be rewritten as follows:

$$H(z) = \sum_{\substack{i=0 \\ \neq((k))_M}}^{M-1} z^{-i} H_i(z^M) + a_K z^{-K}. \qquad (13)$$

A sampling rate in the subfilter $H_i(z^M)$ is the Nyquist rate f_N.

Let $H_i(z^M)$ be

$$H_i(z^M) = P_i(z^M)/Q(z^M). \qquad (14)$$

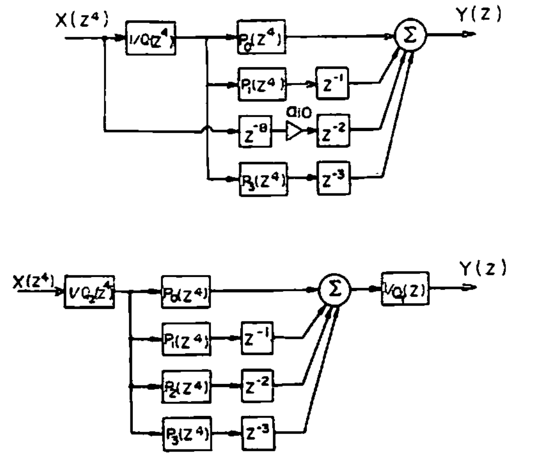

Fig. 2. Optimum configuration for new IIR Nyquist filters, using Nyquist rate subfilters in parallel form. (a) Type A. (b) Type B.

Then

$$P_i(z^M) = \sum_{k=0}^{\left[\frac{N_n - i}{M}\right]} a_{i+kM} z^{-kM} \qquad (15a)$$

$$Q(z^M) = \sum_{k=0}^{\frac{N_d}{M}} b_{kM} z^{-kM}. \qquad (15b)$$

Let the input and output be $X(z^M)$ and $Y(z)$, respectively,

$$Y(z) = \sum_{\substack{i=0 \\ \neq((K))_M}}^{M-1} z^{-i}\left(H_i(z^M)\cdot X(z^M)\right) + a_K z^{-K}\cdot X(z^M). \qquad (16)$$

Signal processing in each subfilter, that is $H_i(z^M)\cdot X(z^M)$, is carried out based on the Nyquist rate f_N. When a denominator is used for all subfilters in common, only one block is required at the input side. Its transfer function is

$$H(z) = \left\{ \sum_{\substack{i=0 \\ \neq((K))_M}}^{M-1} z^{-i} P_i(z^M) \right\} \frac{1}{Q(z^M)} + a_K z^{-K}. \qquad (17)$$

A block diagram to implement (17) is shown in Fig. 2(a).

Type B

One of the denominators $Q_1(z)$, is a polynomial of z^{-1}. Thus Bellanger's method [8] is required in order to break down $H(z)$ into low rate subfilters $H_i(z^M)$. Otherwise, it is necessary to perform the denominator $Q_1(z)$ operation on the sampling rate f_s, after interleaving the output signals from the block consist of $1/Q_2(z^M)$ and the numerator low rate subfilters. In both methods, computational complexity is increased, compared with Type A. The latter transfer function becomes

$$H(z) = \frac{1}{Q_1(z)} \left\{ \sum_{i=0}^{M-1} z_i^{-1} P_i(z^M) \right\} \frac{1}{Q_2(z^M)} \qquad (18)$$

where

$$Q_1(z)=\sum_{j=0}^{M-1} b_j^1 z^{-j} \tag{19a}$$

$$Q_2(z^M)=\sum_{j=0}^{\left[\frac{N_d}{M}\right]} b_{jM} z^{-jM} \tag{19b}$$

$$P_i(z^M)=\sum_{k=0}^{\left[\frac{N_{n-i}}{M}\right]} a_{i+kM} z^{-kM}. \tag{19c}$$

A block diagram for (18) is illustrated in Fig. 2(b).

III. Approximation Procedure in Frequency Domain

The impulse response becomes exactly zero at the Nyquist sampling points except for one point in the proposed IIR Nyquist filters. Time response optimization, therefore, is not required. The transfer function has to be optimized in a frequency domain only. As previously discussed in Section II, Types A and B transfer functions exist. Type A is superior to Type B as regards frequency response optimization and a hardware realization. The impulse response, in Type A, is insensitive at the Nyquist sampling points for finite coefficient and signal wordlengths. Type B, however, gives the sensitive impulse response for both finite wordlengths. Taking into account these considerations for Types A and B, only the former is discussed with respect to the optimization method.

Type A transfer function gives Mth-order pole which is located in both passband and stopband. Hence, the denominator does not contribute to realizing the stopband attenuation. It is used to shape the passband amplitude. The stopband attenuation is mostly realized by the numerator. Considering these properties, the following multistep optimization method is proposed here. First, the numerator is optimized to realize the stopband attenuation under the condition for the numerator coefficients given by the Theorem. Secondarily, the denominator is obtained from the optimized numerator through the condition (8a). Optimization is carried out once more as a whole transfer function to realize the desired stopband attenuation. The optimization algorithm at each step is based on the iterative Chebyshev approximation proposed by Ishizaki–Watanabe [9]. This algorithm efficiency is highly dependent on the initial value for the parameters. A most important problem is how to determine the initial value. A general flow chart is shown in Fig. 3. The detailed algorithm for each step is discussed in the following.

Step 1: Initial Numerator Value.

As discussed in Section II, it is very hard to initialize the dependent zero at the desired location using the independent zero through a few searching steps. So, it is not suitable to initialize the numerator coefficients using the independent zeros only. The aim of the numerator optimization is only to realize the stopband attenuation. The numerator frequency response becomes low Q, in order to accomplish the minimum filter order. Corresponding impulse response, that is coefficient, is broad band. From the given condition, the first half of the numerator coefficient set $\{a_i\}_F$, shown in Fig. 4, has the constraint, that is $a_{K-kM}=0$, $0<k\leq[K/M]$. Therefore, the ideal Nyquist waveform with the given rolloff rate is employed as the initial value for $\{a_i\}_F$, taking into account band-limitation requirement in the frequency domain. On the other hand, the latter half of it, $\{a_i\}_L$, has no constraint in the numerator optimization step. Then the coefficient set of a low Q FIR filter which gives sufficient stopband attenuation, is employed as the initial value for $\{a_i\}_L$. The coefficient value set is scaled so that the maximum value is $1/M$. In addition, the initial value for $\{a_i\}_L$ mostly determines the pole locations in the following steps. Through the iterative Chebyshev approximation used here, the absolute value of a_i is optimized. Its sign, however, is not changed from that for the initial value. An example for the relation between the sign of b_{iM} obtained as a_{K+iM}/a_K, $0<i\leq N_d/M$, and the number of poles located at the phases (radian) 0 and π/M with period $2\pi/M$ is shown in Table I. Two states for the number of poles are considered. One of them is shown with data only, and the other is shown with $(\cdot)$. Since, in actual applications, b_M is sufficiently large compared with both b_{2M} and b_{3M}, poles are mostly located at phases 0 and π/M with period $2\pi/M$. Poles located in the other region are not counted in Table I. The poles located at phase 0 with period $2\pi/M$ are not effectively utilized to optimize the frequency response, because it is canceled by a zero, as shown in the numerical example in Section IV. Thus it is desirable to locate the poles on the phase π/M with period $2\pi/M$ in order to accomplish the minimum filter order.

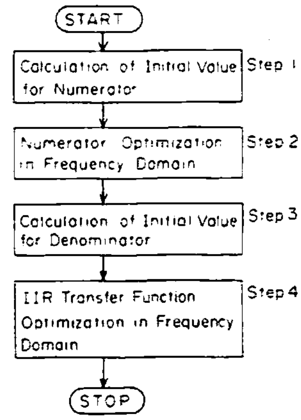

Fig. 3. General flowchart for proposed multistep optimization method.

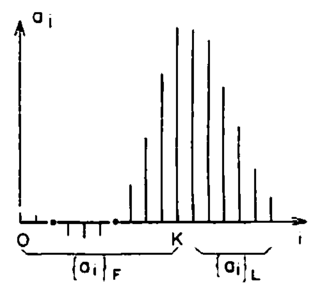

Fig. 4. Example of initial numerator coefficient values in Step 1.

TABLE I
RELATION BETWEEN SIGN OF DENOMINATOR COEFFICIENTS b_{iM} AND POLE LOCATIONS

N_d	b_M	b_{2M}	b_{3M}	Phase (radian) 0	π/M
1 M	+			0	1
2 M	+	+		0	2
	+	−		1	1
3 M	+	+	+	0 (2)	3 (1)
	+	+	−	1	2
	+	−	−	1	2
	+	−	+	0 (2)	3 (1)

The initial value for $\{a_i\}_L$ has to be determined from this point of view.

Step 2: Numerator Optimization.

The numerator $|P(e^{j\omega T})|$ optimization is carried out through the iterative Chebyshev approximation, using the initial value $P^{(1)}(z)$ obtained in Step 1. Letting δ represent the maximum error, a set of linear inequalities can be written to describe this minimax problem

$$W(e^{j0})||P^{(2)}(e^{j0})|-1|<\delta \tag{20a}$$

$$W(e^{j\omega T})\left|\frac{P^{(2)}(e^{j\omega T})}{P^{(2)}(e^{j0})}\right|<\delta, \qquad \pi\frac{f_N}{f_s}(1+\rho/2)\leqslant\omega T\leqslant\pi$$

$$\text{minimize } \delta \tag{20b}$$

where $W(e^{j\omega T})$ is a weighting function. $a_{K-kM}(0<k\leqslant[K/M])$ is fixed to zero during the optimization.

Step 3: Initial Denominator Value.

Initial denominator coefficients are obtained from the optimized numerator $P^{(2)}(z)$ using the following relation:

$$b_{iM}^{(3)}=a_{K+iM}^{(2)}/a_K^{(2)}, \qquad i=1,2,\cdots,\left[\frac{N_n-K}{M}\right]. \tag{21}$$

Furthermore, the initial value for $H^{(3)}(z)$ becomes

$$H^{(3)}(z)=P^{(2)}(z)/Q^{(3)}(z) \tag{22a}$$

where

$$Q^{(3)}(z)=\sum_{i=0}^{\left[\frac{N_n-K}{M}\right]} b_{iM}^{(3)}z^{-iM}. \tag{22b}$$

Step 4: Total Transfer Function Optimization.

The total transfer function is optimized through the same algorithm as that used in Step 2, using the initial value $H^{(3)}(z)$ obtained in Step 3. The minimax problem is basically the same as that in Step 2

$$W(e^{j0})||H^{(4)}(e^{j0})|-1|<\delta \tag{23a}$$

$$W(e^{j\omega T})\left|\frac{H^{(4)}(e^{j\omega T})}{H^{(4)}(e^{j0})}\right|<\delta, \qquad \pi\frac{f_N}{f_s}(1+\rho)\leqslant\omega T\leqslant\pi$$

$$\text{minimize } \delta. \tag{23b}$$

In this step, the parameters are optimized under the Type A conditions given by the Theorem. The optimized $H^{(4)}(z)$ in this step becomes the final solution.

In the proposed design procedure, determining the initial value for the numerator in Step 1 is the most important phase. The Steps 2, 3, and 4 can be automatically carried out. K and N_n are determined by the given rolloff rate ρ, M, and the minimum stopband attenuation A_s. In the actual design procedure, it is necessary to prepare a nomograph for K and N_n, using ρ, M, and A_s as parameters.

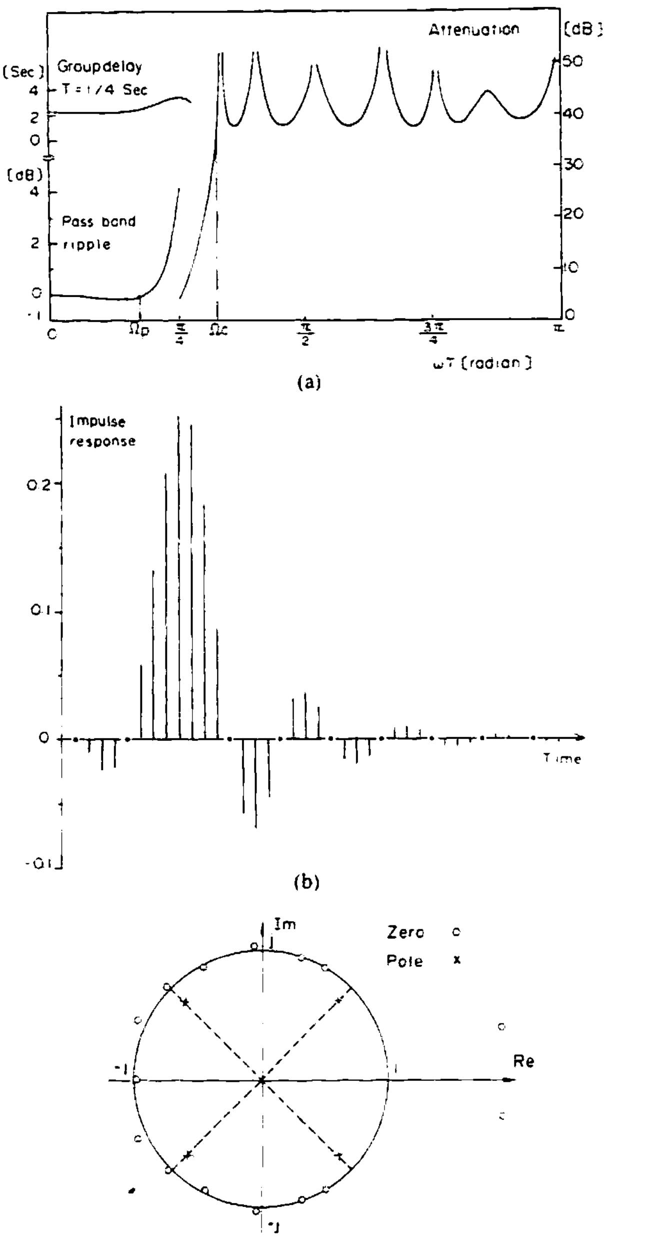

Fig. 5. Design example for new IIR Nyquist filter (Example 1), where $\rho=0.3$, $M=4$, $N_n=15$, $N_d=4$, and $K=9$. (a) Frequency response where, minimum attenuation A_s is 38 dB. (b) Impulse response. (c) Zero-pole locations in z-plane.

IV. DESIGN EXAMPLE AND COMPARISON WITH FIR FILTERS

A. Design Example

Example: 1: $\rho=0.3$(30 percent), $M=4$.

Minimum stopband attenuation of 38 dB is obtained using $K=9$, $N_n=15$, and $N_d=4$. The frequency response, impulse response, and zero-pole locations are shown in Fig. 5. The zero located outside the unit circle in the passband

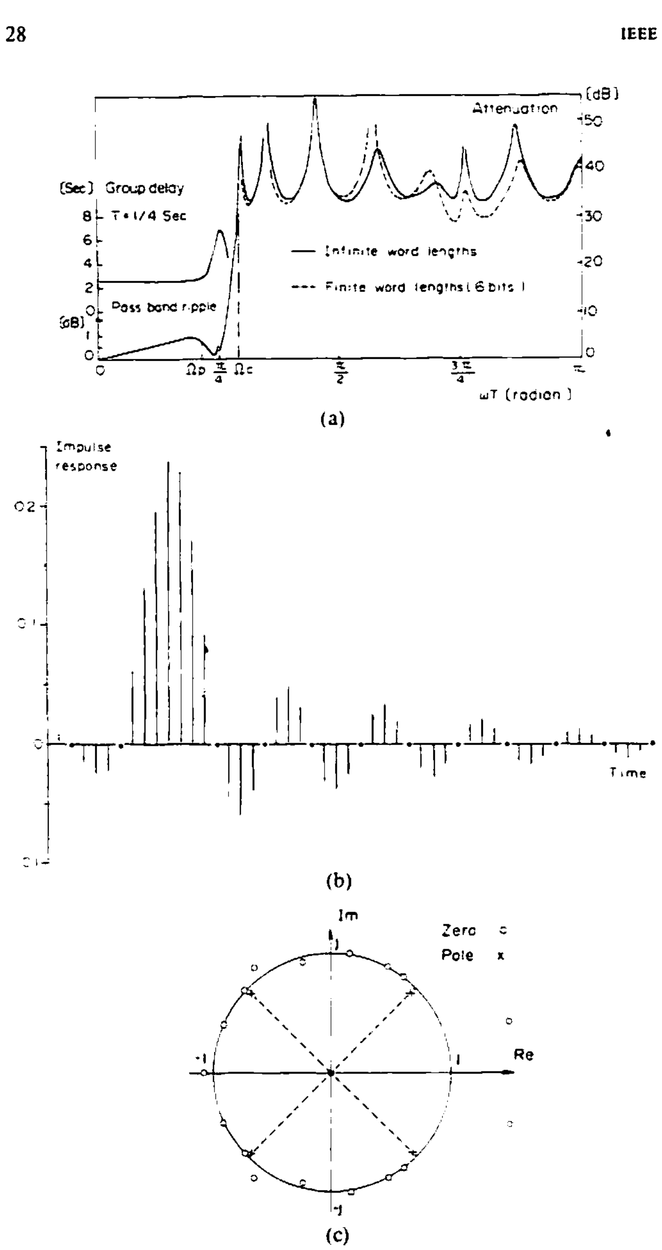

Fig. 6. Design example for new IIR Nyquist filter (Example 2), where $\rho = 0.15$, $M = 4$, $N_n = 17$, $N_d = 4$, and $K = 10$. (a) Frequency response, where $A_s = 33$ dB. (b) Impulse response. (c) Zero-pole locations in z-plane.

can be considered to be utilized for equalizing group delay distortion, as a result. Hence the group delay becomes almost flat in the passband. The numerator and denominator coefficient values are shown in Table II. In this table, the transfer function is taken as (15). Attention has to be paid to the passband loss shaped by the pole located at phase $\pi/4$, nevertheless the passband optimization is not carried out except at $\omega T = 0$ as described in Section III.

Example: 2: $\rho = 0.15$ (15 percent), $M = 4$.

Minimum stopband attenuation of 33 dB is obtained, using $K = 10$, $N_n = 17$, and $N_d = 4$. The results are shown in Fig. 6 and Table III. The attenuation after the coefficient rounding-off are also shown in the same figure. All coefficients are rounded-off into 6 bits (Sign 1 bit, Magnitude 5 bits) after normalizing the maximum value to unity. These wordlengths are called "effective wordlengths" here.

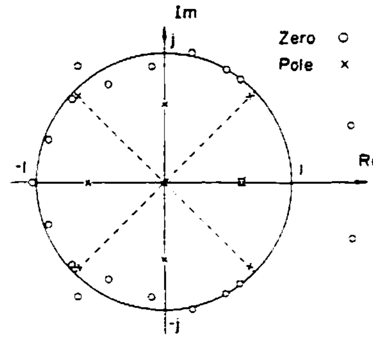

Fig. 7. Zero-pole locations in z-plane for Example 3, where $\rho = 0.15$, $M = 4$, $N_n = 20$, $N_d = 8$, and $K = 10$. A_s is 33 dB.

TABLE II

NUMERATOR AND DENOMINATOR COEFFICIENT VALUES IN EXAMPLE 1. TRANSFER FUNCTION IS BASED ON (15)

a_0	0.006426	a_{10}	0.2762
	—	a_{11}	0.2551
a_2	-0.01186	a_{12}	0.2002
a_3	-0.02312		—
a_4	-0.01994	a_{14}	0.07291
	—	a_{15}	0.02908
a_6	0.05148	a_9	0.2517
a_7	0.1202		
a_8	0.1953	b_0	1.0
	—	b_4	0.5395

TABLE III

NUMERATOR AND DENOMINATOR COEFFICIENT VALUES IN EXAMPLE 2. TRANSFER FUNCTION IS BASED ON (15)

a_0	0.01441	a_{11}	0.2803
a_1	0.009311	a_{12}	0.2791
	—	a_{13}	0.2535
a_3	-0.01620		—
a_4	-0.01420	a_{15}	0.1386
a_5	-0.01543	a_{16}	0.07934
	—	a_{17}	0.03697
a_7	0.04920	a_{10}	0.2375
a_8	0.1099		
a_9	0.1783	b_0	1.0
	—	b_4	0.8140

In the above two examples, the pole is located at phase π/M with period $2\pi/M$. The following example illustrates that a pole located at phase 0 with period $2\pi/M$ is not effectively utilized to optimize the frequency response.

Example: 3: $\rho = 0.15$ (15 percent), $M = 4$.

In this example, the following sign combination; sign $(b_4, b_8) = (+, -)$ is employed in order to locate a pole at phase 0 with period $2\pi/M$. $K = 10$, $N_n = 20$, and $N_d = 8$ have to be required to accomplish the same attenuation as Example 2. the impulse response is almost the same as that for Example 2. The zero-pole locations are shown in Fig. 7. Poles located at phase 0 with period $2\pi/M$ are not effectively utilized for frequency-response optimization, because one of them, located in the passband, is exactly canceled by a zero. This cancellation could be recognized through other examples. Its theoretical analysis has not been accomplished in this paper.

Comparing Examples 2 and 3, it can be recognized that

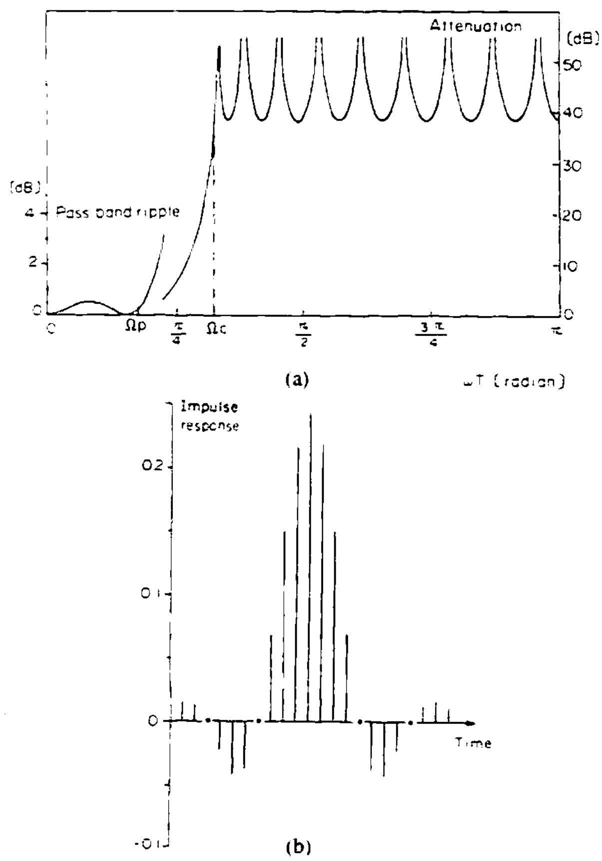

Fig. 8. Design example for FIR Nyquist filter, where $\rho=0.3$, $M=4$, and $N=22$. (a) Frequency response, where $A_s=38$ dB. (b) Impulse response.

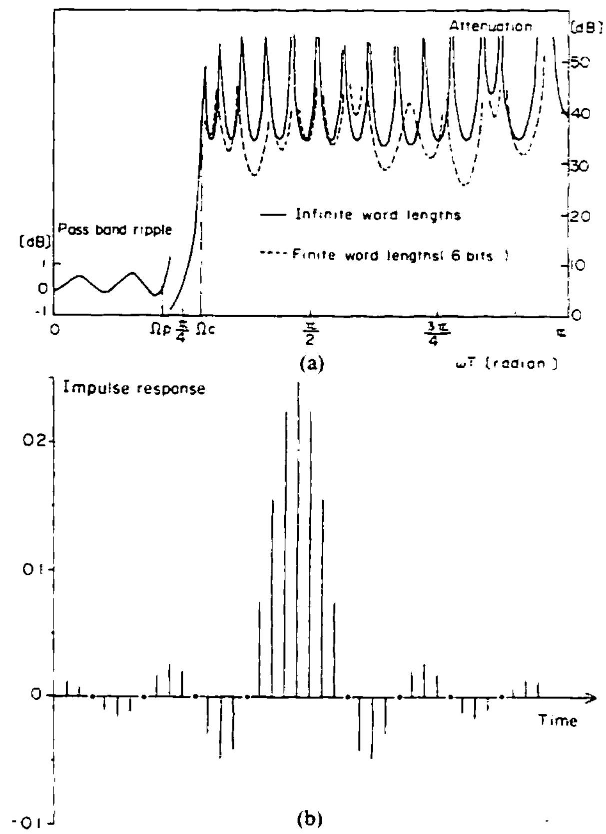

Fig. 9. Design example for FIR Nyquist filter, where $\rho=0.15$, $M=4$, and $N=38$. (a) Frequency response, where $A_s=33$ dB. (b) Impulse response.

locating poles at phase π/M with period $2\pi/M$ is useful for minimizing the filter order. Zero-pole locations in the Type B transfer function correspond to that of Fig. 7 after removing the pole and zero which cancel each other at phase 0. Type B can be recognized not to offer the optimum zero-pole location compared with Type A in Fig. 6.

B. Comparison Between the New IIR and the FIR Nyquist Filters

The conventional method to realize zero intersymbol interference is FIR Nyquist filters. Their comparison, based on filter order and computational complexity, is discussed here. A two-step design method using the Remez-exchange [10] and the iterative Chebyshev approximation has been proposed [11], and is employed here. The design procedure is explained briefly in the following.

Step 1: Remez-Exchange Approximation.

Let $H(z)$ be a transfer function for FIR Nyquist filters

$$H(z)=\sum_{n=0}^{N} h_n z^{-n}. \tag{24}$$

$H(z)$ is approximated through the well-known Remez-exchange algorithm. Let $D(e^{j\omega T})$ be the desired frequency response. In this step, $|D(e^{j\omega T})|$ takes the following values:

$$|D(e^{j\omega T})|=1, \qquad 0\leq \omega T\leq \pi\frac{f_N}{f_s}(1-\rho) \tag{25a}$$

$$=0.5, \qquad \omega T=\pi f_N/f_s \tag{25b}$$

$$=0, \qquad \pi\frac{f_N}{f_s}(1+\rho)\leq \omega T\leq \pi. \tag{25c}$$

Step 2: Iterative Chebyshev Approximation.

The result in the previous step is taken as the initial value for $H^{(2)}(z)$, and h_i is modified to zero for $((i-K))_M=0$ and $i\neq K$. The minimax problem is also represented as follows:

$$W(e^{j0})||H^{(2)}(e^{j0})|-1|<\delta \tag{26a}$$

$$W(e^{j\omega T})\left|\frac{H^{(2)}(e^{j\omega T})}{H^{(2)}(e^{j0})}\right|<\delta, \qquad \pi\frac{f_N}{f_s}(1+\rho)\leq \omega T\leq \pi$$

$$\text{minimize } \delta. \tag{26b}$$

Design examples for FIR Nyquist filters, realizing the same minimum stopband attenuations as the IIR type, are shown in Figs. 8 and 9. Filter sizes become 23 and 39 taps for 30- and 15-percent rolloff rates, respectively. Hardware size for the IIR Nyquist filters can be reduced to 74 and 52 percent of that for the FIR Nyquist filters, based on the previously described parallel form using the low rate subfilters. Advantage cannot be used of the coefficient symmetry in FIR filters for the parallel form. The group delay, in the IIR approach, is significantly reduced. It can be also recognized that the IIR Nyquist filter efficiency becomes more marked for high Q Nyquist filters.

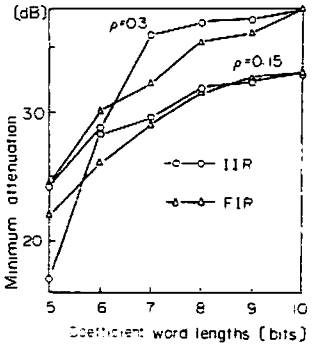

Fig. 10. Minimum attenuation in stopband caused by rounded-off coefficients. Coefficient wordlengths are expressed as effective wordlengths.

Sensitivity

The minimum attenuations in the stopband caused by the rounded-off coefficients for both IIR and FIR filters are shown in Fig. 10. They are almost the same except for the shortest wordlengths. The minimum attenuation appears around $\omega T=\pi/M$ with $.2\pi/M$ in the IIR Nyquist filters as shown in Fig. 6(a). On the other hand, Fig. 9(a) shows that it appears at many frequency points in the FIR Nyquist filters. So, the average attenuation in the stopband for the IIR approach is superior to that for the FIR approach.

Scaling and Roundoff Noise

The IIR Nyquist filter illustrated in Fig. 2(a) requires the input signal scaling to prevent overflows in the denominator block. The scaling factors evaluated by the L_∞ norms become 0.46 and 0.19 in the Examples 1 and 2, respectively. The FIR Nyquist filters do not require the input scaling in a direct form. The output roundoff noise in the FIR type is a little larger than that for the IIR type, the difference, however, is within 1 bit regards as signal wordlengths.

V. Conclusion

A new IIR Nyquist filter with zero intersymbol interference is proposed. Necessary and sufficient conditions for a transfer function are obtained. A multistep design method, based on the iterative Chebyshev approximation, is proposed. This method makes it possible to design a new kind of IIR Nyquist filter with the minimum order. Numerical examples for 30- and 15-percent rolloff rates are illustrated. From these examples, it is confirmed that the proposed IIR Nyquist filter can reduce the filter order and hardware size, compared with conventional FIR Nyquist filters. Its efficiency is remarkable for high Q Nyquist filters.

Appendix

Proof of Theorem

Let $P(z)$ and $Q(z)$ be a numerator and a denominator polynomials, respectively. $H(z)$ can be expanded using h_n as follows:

$$H(z)=\frac{P(z)}{Q(z)}=\frac{\sum_{i=0}^{N_n} a_i z^{-i}}{\sum_{i=0}^{N_d} b_i z^{-i}}=\sum_{n=0}^{\infty} h_n z^{-n}. \quad \text{(A1)}$$

Equation (A1) can be written

$$\sum_{i=0}^{N_n} a_i z^{-i}\left(\sum_{i=0}^{N_d} b_i z^{-i}\right)\left(\sum_{n=0}^{\infty} h_n z^{-n}\right). \quad \text{(A2)}$$

Since (A2) is the identity of z, the relation between a_i, b_i, and h_n can be obtained by comparing the coefficients of the same power of z^{-1} in both sides of (A2). Necessary and sufficient conditions are proved based on this relation.

(Necessary Condition)
Denominator Coefficients

From (A2), the following relation between b_i and h_i is obtained

$$\begin{bmatrix} h_{N-1} & h_{N-2} & \cdots & h_{N-N_d} \\ h_{N+M-1} & h_{N+M-2} & \cdots & h_{N+M-N_d} \\ \vdots & \vdots & \ddots & \vdots \\ h_{N+(N_d-1)M-1} & h_{N+(N_d-1)M-2} & \cdots & h_{N+(N_d-1)M-N_d} \end{bmatrix} \cdot \begin{bmatrix} b_1 \\ b_2 \\ \vdots \\ b_{N_d} \end{bmatrix} = -\begin{bmatrix} h_N \\ h_{N+M} \\ \vdots \\ h_{N+(N_d-1)M} \end{bmatrix} \quad \text{(A3a)}$$

where

$$N_n < N-1. \quad \text{(A3b)}$$

In (A3), N is taken so as to satisfies (A4)

$$K < N - N_d \quad \text{(A4a)}$$

$$((N-K))_M = 0. \quad \text{(A4b)}$$

Using the h_n property given by (5), the right-hand side of (A3) becomes $(0,0,\cdots,0)^t$, and the iMth ($i=1,2,\cdots,[N_d/M]$) row in the coefficient matrix also becomes $(0,0,\cdots,0)^t$. Equation (A3) is reduced by removing the iMth row in the coefficient matrix, and b_{iM} in the vector $(b_1, b_2,\cdots, b_{N_d})^t$, and expressed as follows:

$$H_0 \boldsymbol{b}_0 = \boldsymbol{h}_0 \quad \text{(A5)}$$

where sizes for H_0, $\boldsymbol{b}_0$, and $\boldsymbol{h}_0$ are $(N_d-[N_d/M])\times(N_d-[N_d/M])$, $N_d-[N_d/M]$ and $N_d-[N_d/M]$, respectively. Equation (A5) has different solutions for the N_d value. Therefore, (A5) solving is carried out for three kinds of the N_d values.

(i)
$$0<((N_d))_M < M-1. \quad \text{(A6)}$$

There exists the following linear dependency:

$$h_{N-1+jM} = -\sum_{i=1}^{N_d} h_{N-1+jM-i}\cdot b_i, \qquad j=0,1,\cdots,N_{d-1}. \quad \text{(A7)}$$

If $b_{N_d} \neq 0$, h_n other than the elements of the set $\{h_n | n = N + jM - 2, \cdots, N + jM - N_d\}$ has to be required to express h_{N-1+jM} as the linear combination of h_n. It means that the linear dependency does not exist in the H_0 matrix, and

$$\det H_0 \neq 0. \tag{A8}$$

Since $\boldsymbol{h}_0$ is a zero vector in (A5)

$$\boldsymbol{b}_0 = 0. \tag{A9}$$

As a result, b_{N_d} becomes zero, and is not consistent with the above condition.It means that (A6) cannot become the necessary condition for the given h_n.

(ii)
$$((N_d))_M = 0. \tag{A10}$$

From the same reason as the above state, the H_0 matrix rank becomes $N_d - N_d/M$, and $\boldsymbol{b}_0$ also becomes zero. In this case, however, $\boldsymbol{b}_0$ does not contain b_{N_d} because of $((N_d))_M = 0$. If $b_{N_d} \neq 0$, the nonzero solution, satisfies (A3), exists. Therefore, $\boldsymbol{b}_0 = 0$ is the necessary condition for b_i.

(iii)
$$((N_d))_M = M - 1. \tag{A11}$$

h_n has the following linear dependency:

$$h_{N-1+jM} = -\sum_{i=1}^{N_d-1} h_{N-1+jM-i} \cdot b_i, \qquad j = 0, 1, \cdots, N_{d-1} \tag{A12}$$

because $h_{N-1+jM-i}$ is zero for $i = N_d$. Equation (A12) means h_{N-1+jM} is expressed as the linear combination of h_n $(n = N + jM - 2, \cdots, N + jM - N_d)$. Therefore, the H_0 matrix rank becomes less than $N_d - [N_d/M]$, and

$$\det H_0 = 0. \tag{A13}$$

In this case, $\boldsymbol{b}_0$ becomes an uncertain solution because $\boldsymbol{h}_0$ is a zero vector. Equation (A13) is equivalent to the following linear dependency:

$$\sum_{i=0}^{N_d-1} h_{N-1+jM-i} \cdot b_{i+1} = 0, \qquad j = 0, 1, \cdots, N_{d-1}. \tag{A14}$$

Equation (A14) is equivalent to (A12). Comparing both linear dependencies on the h_n, the necessary condition for b_i can be obtained.

If

$$b_1 \neq 0 \tag{A15}$$

(A14) can be rewritten as follows:

$$h_{N-1+jM} = -\frac{1}{b_1} \sum_{i=1}^{N_d-1} h_{N-1+jM-i} b_{i+1}. \tag{A16}$$

From (A12), and the h_n condition, b_i can be expressed as follows:

$$b_i = b_{M[\frac{i}{M}]} b_1^{((i))_M}. \tag{A17}$$

Let l be the minimum integer satisfying $b_l = 0$. When $1 \leq l$, the reduced coefficient matrix of (A5) obtained by removing the ith $(i = 1, \cdots, l)$ row, does not have the linear dependency, and its rank is full. b_{N_d} becomes zero, and the N_d condition cannot be satisfied.

Consequently. (A5)'s solutions are given by either (A10) and (A9) or (A11) and (A17). They become also the necessary conditions for the b_i to satisfy (5).

Numerator Coefficients

The numerator coefficients a_i can be expressed using b_i and h_i, based on (A2) as follows:

$$\begin{bmatrix} a_0 \\ a_1 \\ \vdots \\ a_{N_n} \end{bmatrix} = \begin{bmatrix} h_0 & 0 & \cdots & 0 \\ h_1 & h_0 & \ddots & \vdots \\ \vdots & \vdots & \ddots & 0 \\ & & & h_0 \\ & & & \vdots \\ h_{N_n} & h_{N_n-1} & \cdots & h_{N_n-N_d} \end{bmatrix} \cdot \begin{bmatrix} 1 \\ b_1 \\ \vdots \\ b_{N_d} \end{bmatrix} \tag{A18a}$$

where $N_d \leq N_n$ or

$$\begin{bmatrix} a_0 \\ a_1 \\ \vdots \\ a_{N_n} \end{bmatrix} = \begin{bmatrix} h_0 & 0 & \cdots & & & 0 \\ h_1 & h_0 & \ddots & & & \vdots \\ \vdots & \vdots & \ddots & & & \\ h_{N_n-1} & h_{N_n-1} & h_0 & 0 & \cdots & 0 \end{bmatrix} \cdot \begin{bmatrix} 1 \\ b_1 \\ \vdots \\ b_{N_d} \end{bmatrix} \tag{A18b}$$

where $N_d > N_n$.

Type A

a_{K-kM}, $(k > 0)$ can be expressed as follows:

$$a_{K-kM} = \sum_{i=0}^{N_d} h_{K-kM-i} \cdot b_i. \tag{A19}$$

In this case $b_i = 0$, $((i))_M \neq 0$, then

$$a_{K-kM} = \sum_{i=0}^{\frac{N_d}{M}} h_{K-kM-iM} \cdot b_{iM}. \tag{A20}$$

From the condition for h_n: $h_{K-kM-iM} = 0$, the following condition is obtained:

$$a_{K-kM} = 0 \tag{A21}$$

a_K is expressed as follows:

$$a_K = \sum_{i=0}^{\frac{N_d}{M}} h_{K-iM} b_{iM}. \tag{A22}$$

Using the h_n property,

$$a_K = h_K b_0 = h_K \tag{A23}$$

then it is necessary that a_K becomes nonzero

$$a_K \neq 0. \tag{A24}$$

a_{K+kM}, $(k > 0)$ is expressed as follows:

$$a_{K+kM} = \sum_{i=0}^{\frac{N_d}{M}} h_{K+kM-iM} b_{iM}. \tag{A25}$$

From (A21) and (A24),

$$a_{K+kM}=a_K b_{kM}, \qquad k=1,2,\cdots,\frac{N_d}{M} \tag{A26a}$$

and

$$a_{K+kM}=0, \frac{N_d}{M}<k. \tag{A26b}$$

Equations (A21), (A24), and (A26) are the necessary conditions for the a_i in Type A.

Type B

From (A17) the denominator can be broken down into two factors

$$Q(z)=\left(\sum_{k=0}^{\left[\frac{N_d}{M}\right]} b_{kM}z^{-kM}\right)\left(\sum_{j=0}^{M-1} b_1^j z^{-j}\right). \tag{A27}$$

a_i is expressed as the convolution of b_i and h_n. Using the factorized denominator, a_i is obtained by two convolution steps as follows:

$$a_i=\sum_{k=0}^{\left[\frac{N_d}{M}\right]} b_{kM}\sum_{j=0}^{M-1} h_{i-kM-j}\cdot b_1^j. \tag{A28}$$

$a_i-a_{i-1}\cdot b_1$ can be expressed using h_{i-kM} $(0\leq k)$ and h_i:

$$a_i-a_{i-1}\cdot b_1$$
$$=\sum_{k=0}^{\left[\frac{N_d}{M}\right]} b_{kM}\sum_{j=0}^{M-1}\left(h_{i-kM-j}\cdot b_1^j-h_{i-1-kM-j}\cdot b_1^{j+1}\right) \tag{A29a}$$
$$=\sum_{k=0}^{\left[\frac{N_d}{M}\right]} b_{kM}\left(h_{i-kM}-h_{i-(k+1)M}\cdot b_1^M\right) \tag{A29b}$$
$$=h_i+\sum_{k=1}^{\left[\frac{N_d}{M}\right]+1}\left(b_{kM}-b_{(k-1)M}\cdot b_1^M\right)h_{i-kM}. \tag{A29c}$$

Applying the h_n conditions to (A29c) the following necessary conditions for the a_i are obtained:

$$a_{K-kM}-a_{K-kM-1}\cdot b_1=0, \qquad 1\leq k\leq\left[\frac{K}{M}\right] \tag{A30a}$$
$$a_K-a_{K-1}\cdot b_1=h_K\neq 0 \tag{A30b}$$
$$a_{K+kM}-a_{K+kM-1}\cdot b_1=\left(b_{kM}-b_{(k-1)M}\cdot b_1^M\right)\cdot\left(a_K-a_{K-1}\cdot b_1\right). \tag{A30c}$$

(Sufficient Condition)

Type A: $((N_d))_M=0$.

Let h_n^Q be the impulse response of the denominator $1/Q(z)$. Since $Q(z)$ is a polynomial of z^{-M}, then h_n^Q satisfies the following equation:

$$h_n^Q=0, \qquad ((n))_M\neq 0. \tag{A31}$$

The impulse response for $H(z)$ can be obtained as the convolution of h_n^Q and a_i

$$h_n=\sum_{i=0}^{N_n} a_i h_{n-i}^Q. \tag{A32}$$

h_K is expressed as follows:

$$h_K=\sum_{i=0}^{N_n} a_i h_{K-i}^Q. \tag{A33}$$

From (A31)

$$h_K=\sum_{j=0}^{\left[\frac{K}{M}\right]} a_{K-jM}h_{jM}^Q. \tag{A34}$$

Using (A21), h_K becomes

$$h_K=a_K. \tag{A35}$$

From (A24), that is $a_K\neq 0$, (5c) is satisfied

$$h_{K-kM}=\sum_{i=0}^{N_n} a_i h_{K-kM-i}^Q, \qquad k>0. \tag{A36}$$

Using (A31)

$$h_{K-kM}=\sum_{j=0}^{\left[\frac{K-kM}{M}\right]} a_{K-kM-jM}h_{jM}^Q. \tag{A37}$$

Applying (A21)

$$h_{K-kM}=0. \tag{A38}$$

The first half of (5b), where a_K is the border, is satisfied.

$$h_{K+kM}=\sum_{i=0}^{N_n} a_i h_{K+kM-i}^Q, \qquad k>0 \tag{A39a}$$
$$=\sum_{j=0}^{\left[\frac{K+kM}{M}\right]} a_{K+kM-jM}\cdot h_{jM}^Q. \tag{A39b}$$

Using (A26)

$$h_{K+kM}=\sum_{j=0}^{k} a_K b_{(k-j)M}\cdot h_{jM}^Q \tag{A40a}$$
$$=0 \tag{A40b}$$

because h_{jM}^Q satisfies the following relation:

$$\sum_{j=0}^{k} b_{(k-j)M}\cdot h_{jM}^Q=0, \qquad 0<k. \tag{A41}$$

The latter half of (5) is satisfied. The necessary conditions given by (A9), (A10), (A21), (A24), and (A26) are proved to be sufficient conditions. They are summarized as (6), (7), and (8) in the theorem.

Type B $((N_d))_M=M-1$

The denominator $Q(z)$ is broken down into two factors, as shown in (A27), thus:

$$Q(z)=\left(\sum_{k=0}^{\left[\frac{N_d}{M}\right]} b_{kM}z^{-kM}\right)\left(\sum_{j=0}^{M-1} b_1^j z^{-j}\right). \tag{A27}$$

Let the first and second terms be $Q_1(z)$ and $Q_2(z^M)$, respectively. $Q_1(z)$ can be rewritten as follows:

$$\frac{1}{Q_1(z)} = \frac{1-b_1z^{-1}}{1-b_1^M z^{-M}}. \quad \text{(A42)}$$

The impulse response q_n^* for $1/(1-b_1^M z^{-M})$ satisfies

$$q_n^* = b_1^n, \quad ((n))_M = 0 \quad \text{(A43a)}$$

$$= 0, \quad ((n))_M \neq 0. \quad \text{(A43b)}$$

The impulse response q_n for $1/Q_1(z)$ is

$$q_n = q_n^* - b_1 q_{n-1}^*. \quad \text{(A44)}$$

Applying (A43)

$$q_n = \mu_n (-1)^{((n))_M} \cdot b_1^n \quad \text{(A45)}$$

where

$$\mu_n = 1, \quad ((n))_M = 0, 1 \quad \text{(A46a)}$$

$$= 0, \quad ((n))_M = 2, 3, \cdots, M-1, \text{ and } n < 0. \quad \text{(A46b)}$$

The impulse response h_n^* for $P(z)/Q_1(z)$ is expressed using q_n and (A45)

$$h_n^* = \sum_{i=0}^{N_n} a_i q_{n-i} \quad \text{(A47a)}$$

$$= \sum_{i=0}^{N_n} a_i \mu_{n-i} (-1)^{((n-i))_M} \cdot b_1^{n-i}. \quad \text{(A47b)}$$

The impulse response h_n for $H(z) = P(z)/Q(z)$ is obtained as the convolution of h_n^* and the $1/Q_2(z^{-M})$ impulse response as follows:

$$h_n = h_n^* - \sum_{l=1}^{\left[\frac{N_d}{M}\right]} h_{n-lM} b_{lM}. \quad \text{(A48)}$$

h_n^* is calculated at first, and h_n is obtained by (A48) using h_n^*.

From (A47) $h_{K-kM}^* \cdot (0<k)$ becomes

$$h_{K-kM}^* = \sum_{i=0}^{K-kM} a_i \mu_{K-kM-i} (-1)_M^{((K-kM-i))} \cdot b_1^{K-kM-i}. \quad \text{(A49)}$$

Applying (A46)

$$h_{K-kM}^* = \sum_{m=0}^{\left[\frac{K-kM}{M}\right]} (a_{K-kM-mM} - a_{K-kM-mM-1} \cdot b_1) b_1^{mM}. \quad \text{(A50)}$$

From the necessary condition for the a_i, that is (A30)

$$h_{K-kM}^* = 0 \quad \text{(A51)}$$

h_K^* is

$$h_K^* = \sum_{i=0}^{K} a_i \mu_{K-i} (-1)^{((K-i))_M} b_1^{K-i} \quad \text{(A52a)}$$

$$= a_K - a_{K-1} \cdot b_1 \quad \text{(A52b)}$$

$$\neq 0. \quad \text{(A52c)}$$

$h_{K+kM}^* \cdot (0<k)$ is

$$h_{K+kM}^* = \sum_{i=0}^{K+kM} a_i \mu_{K+kM-i} (-1)^{((K+kM-i))_M} \cdot b_1^{K+kM-i} \quad \text{(A53a)}$$

$$= \sum_{j=0}^{k} (a_{K+jM} - a_{K+jM-1} \cdot b_1) b_1^{(k-j)M}. \quad \text{(A53b)}$$

From (A30) h_{K+kM}^* becomes

$$h_{K+kM}^* = \sum_{j=0}^{k} \left(b_{jM} - b_{(j-1)M} b_1^M\right) h_K \cdot b_1^{(k-j)M} \quad \text{(A54)}$$

and can be rewritten as follows:

$$h_{K+kM}^* = h_K b_{kM}, \quad 0 \leq k \leq \left[\frac{N_d}{M}\right] \quad \text{(A55a)}$$

$$h_{K+kM}^* = 0, \quad \left[\frac{N_d}{M}\right] < k. \quad \text{(A55b)}$$

h_n is obtained through (A48) using the above results.

$$h_{K-kM} = h_{K-kM}^* - \sum_{l=1}^{\left[\frac{N_d}{M}\right]} h_{K-kM-lM} \cdot b_{lM}. \quad \text{(A56)}$$

From (A51) h_{K-kM} becomes also zero

$$h_{K-kM} = 0, \quad 0 < k \quad \text{(A57)}$$

$$h_K = h_K^* - \sum_{l=1}^{\left[\frac{N_d}{M}\right]} h_{K-lM} \cdot b_{lM}. \quad \text{(A58)}$$

From (A52) and (A57)

$$h_K = h_K^* \neq 0 \quad \text{(A59)}$$

$$h_{K+kM} = h^*_{K+kM} - \sum_{l=1}^{\left[\frac{N_d}{M}\right]} h_{K+kM-lM} \cdot b_{lM}. \quad \text{(A60)}$$

h_{K+M} is obtained at first

$$h_{K+M} = h_{K+M}^* - \sum_{l=1}^{\left[\frac{N_d}{M}\right]} h_{K+M-lM} \cdot b_{lM} \quad \text{(A61a)}$$

$$= h_{K+M}^* - h_K \cdot b_M. \quad \text{(A61b)}$$

Using (A55)

$$h_{K+M} = h_K b_M - h_K b_M$$

$$= 0. \quad \text{(A62)}$$

$h_{K+kM} \cdot (0<k)$ is obtained sequentially starting from h_{K+M} as follows:

$$h_{K+kM} = h_{K+kM}^* - h_K b_{kM}, \quad 1 \leq k \leq \left[\frac{N_d}{M}\right] \quad \text{(A63a)}$$

$$h_{K+kM} = h_{K+kM}^*, \left[\frac{N_d}{M}\right] < k \quad \text{(A63b)}$$

at the same time (A64) is obtained

$$h_{K+kM}=0, \qquad 0<k. \tag{A64}$$

Consequently, the h_n conditions are satisfied, and the necessary conditions for the b_i and the a_i given by (A11), (A15), (A17), and (A30) are proved to be sufficient conditions. They are summarized as (9), (10), and (11). Q.E.D.

Acknowledgment

The authors thank M. Hibino for his useful discussions.

References

[1] D. A. Spaulding, "Synthesis of pulse-shaping networks in the time domain," *Bell Syst. Tech. J.*, vol. 48, pp. 2425–2444, Sept. 1969.

[2] G. C. Temes and M. Gyi, "Design of filters with arbitrary passband and Chebyshev stopband attenuation," in *IEEE Int. Convention Dig.*, Mar. 1967.

[3] N. Yoshida and Y. Ishizaki, "A transfer function with prescribed minimum effective stopband loss and its time response approximation (in Japanese)," *IECE of Japan, Trans.* vol. 54-A, pp. 466–473, Aug. 1971.

[4] M. Hibino, "IIR low-pass filters with specified equiripple stopband loss and its time response approximation (in Japanese)," *IECE of Japan Trans.* vol. J62-A, pp. 895–902, Dec. 1979.

[5] K. H. Mueller, "A new approach to optimum pulse shaping in sampled systems using time-domain filtering," *Bell Syst. Tech. J.*, vol. 52, pp. 723–729, May–June 1973.

[6] D. W. Burlage, R. C. Houts, and G. L. Vaughn, "Time-domain design of frequency-sampling digital filters for pulse shaping using linear programming techniques," *IEEE Trans. Acoust., Speech, Signal Processing*, vol. ASSP-22, pp. 180–185, June 1974.

[7] K. Feher and R. D. Cristogaro, "Transversal filter and application in satellite communications," *IEEE Trans. Commun.*, vol. COM-24, pp. 1262–1268, Nov. 1976.

[8] M. Bellanger and J. L. Daguet, "TDM-FDM transmultiplexers: Digital polyphase and FFT," *IEEE Trans. Commun.* vol. COM-22, pp. 1199–1205, Sept. 1974.

[9] Y. Ishizaki and H. Watanabe, "An iterative Chebyshev approximation method for network design," *IEEE Trans. Circuit Theory*, vol. CT-15, pp. 326–336, Dec. 1968.

[10] T. W. Parks and J. H. McClellan, "Chebyshev approximation for nonrecursive digital filters with linear phase," *IEEE Trans. Circuit Theory*, vol. CT-19, pp. 189–194, Mar. 1972.

[11] M. Hibino, T. Mizukami and K. Nakayama, "A design of FIR filters with zero intersymbol interference (in Japanese)," *IECE of Japan, National Convention Rec. 1799*, Mar. 1980.

Kenji Nakayama (M'73) was born in Mie Prefecture, Japan, on February 24, 1947. He received the B.E. degree in electronics engineering from the Tokyo Institute of Technology, Tokyo, Japan, in 1971.

From 1971 to 1972 he was engaged in research at the T. I. T. Since he joined Transmission Division, Nippon Electronic Company, Ltd. in 1972, he has worked on the research and development of LC, digital and switched-capacitor filters. His current research interests are in the areas of digital signal processing and network theory.

Mr. Nakayama is a member of the Institute of Electronics and Communication Engineering of Japan.

Toshihiko Mizukami was born in Gifu-Pref., Japan, on October 21, 1951. He received the B.E. degree in electrical engineering from Nagoya University, Nagoya, Japan, in 1974.

Since he joined Transmission Division, Nippon Electric Company, Ltd. in 1974, he has worked on the application of digital filters in communication systems. His current interests are in speech recognition and digital signal processing.

Mr. Mizukami is a member of the Institute of Electronics and Communication Engineering of Japan.